



# Karbala International Journal of Modern Science

Manuscript 3378

## Photoluminescence Intensity Enhancement and Stability in CdTe/SiO<sub>2</sub> Quantum Dots through Water Molecule Adsorption and Trap Passivation

Daniil S. Daibagya

Ivan A. Zakharchuk

Sergei A. Ambrozevich

Mikhail S. Smirnov

Anna V. Osadchenko

See next page for additional authors

Follow this and additional works at: <https://kijoms.uokerbala.edu.iq/home>



Part of the [Biology Commons](#), [Chemistry Commons](#), [Computer Sciences Commons](#), and the [Physics Commons](#)



University of  
**Kerbala**

---

# Photoluminescence Intensity Enhancement and Stability in CdTe/SiO<sub>2</sub> Quantum Dots through Water Molecule Adsorption and Trap Passivation

## Abstract

The study of the luminescence photostability for colloidal nanocrystals is an important task since the understanding of the corresponding physical processes advances new electronic devices based on semiconductor nanoparticles as well as other important applications such as biomarkers. In this paper, we provide the first study and comprehensive analysis of the photostability of the luminescent properties for colloidal CdTe/SiO<sub>2</sub> core/shell quantum dots prepared by an aqueous-based method. The quantum dots were exposed to continuous laser radiation during two time intervals with prolonged break in between. The photoluminescence intensity of the quantum dots increased over time under continuous laser irradiation. Also, some processes occurred in the quantum dots in the dark (during the break), leading to a further increase in the photoluminescence intensity after turning on the laser radiation in the second time interval. The observed continuous photoluminescence intensity enhancement of the CdTe/SiO<sub>2</sub> quantum dots was attributed to adsorption of water molecules on the surface of the nanocrystals and, as a consequence, to a decrease in the probability of nonradiative transitions. The positions of the photoluminescence intensity maximum and the colorimetric characteristics have been found to be stable against prolonged laser irradiation. This has been explained by the fact that for the CdTe core capped with a large-bandgap SiO<sub>2</sub> shell (with respect to the bandgap of CdTe), photocorrosion, which is often responsible for the PL blueshift, is a slow process. The results of our work can be used in the development of optoelectronic and nanophotonic devices based on colloidal CdTe/SiO<sub>2</sub> nanostructures.

## Keywords

Photoluminescence intensity enhancement; nanoparticles; Nanocrystals; CdTe/SiO<sub>2</sub>; Traps

## Creative Commons License



This work is licensed under a [Creative Commons Attribution-Noncommercial-No Derivative Works 4.0 License](https://creativecommons.org/licenses/by-nc-nd/4.0/).

## Authors

Daniil S. Daibagya, Ivan A. Zakharchuk, Sergei A. Ambrozevich, Mikhail S. Smirnov, Anna V. Osadchenko, Oleg V. Ovchinnikov, and Alexandr S. Selyukov

## RESEARCH PAPER

# Photoluminescence Intensity Enhancement and Stability in CdTe/SiO<sub>2</sub> Quantum Dots Through Water Molecule Adsorption and Trap Passivation

Daniil S. Daibagya <sup>a,b,\*</sup>, Ivan A. Zakharchuk <sup>a,b</sup>, Sergei A. Ambrozevich <sup>a,b</sup>, Mikhail S. Smirnov <sup>c</sup>, Anna V. Osadchenko <sup>a,b</sup>, Oleg V. Ovchinnikov <sup>c</sup>, Alexandr S. Selyukov <sup>a</sup>

<sup>a</sup> P.N. Lebedev Physical Institute of the Russian Academy of Sciences, Moscow, Russian Federation

<sup>b</sup> Bauman Moscow State Technical University, Moscow, Russian Federation

<sup>c</sup> Voronezh State University, Voronezh, Russian Federation

## Abstract

The study of the luminescence photostability for colloidal nanocrystals is an important task since the understanding of the corresponding physical processes advances new electronic devices based on semiconductor nanoparticles as well as other important applications such as biomarkers. In this paper, we provide the first study and comprehensive analysis of the photostability of the luminescent properties for colloidal CdTe/SiO<sub>2</sub> core/shell quantum dots prepared by an aqueous-based method. The quantum dots were exposed to continuous laser radiation during two time intervals with prolonged break in between. The photoluminescence intensity of the quantum dots increased over time under continuous laser irradiation. Also, some processes occurred in the quantum dots in the dark (during the break), leading to a further increase in the photoluminescence intensity after turning on the laser radiation in the second time interval. The observed continuous photoluminescence intensity enhancement of the CdTe/SiO<sub>2</sub> quantum dots was attributed to adsorption of water molecules on the surface of the nanocrystals and, as a consequence, to a decrease in the probability of nonradiative transitions. The positions of the photoluminescence intensity maximum and the colorimetric characteristics have been found to be stable against prolonged laser irradiation. This has been explained by the fact that for the CdTe core capped with a large-bandgap SiO<sub>2</sub> shell (with respect to the bandgap of CdTe), photocorrosion, which is often responsible for the PL blueshift, is a slow process. The results of our work can be used in the development of optoelectronic and nanophotonic devices based on colloidal CdTe/SiO<sub>2</sub> nanostructures.

**Keywords:** Photoluminescence intensity enhancement, Nanoparticles, Nanocrystals, CdTe/SiO<sub>2</sub>, Traps

## 1. Introduction

Colloidal semiconductor nanocrystals such as quantum dots (QDs) [1–8], nanowires [9–11], nanoplatelets [12–16], and nanoscrolls [17,18] have attracted much attention due to the quantum confinement effect, which provides them with unique linear and nonlinear properties [19–23], which are governed by the average size of the

nanocrystals [24,25]. QDs are of particular interest since excitons are confined in three dimensions. Colloidal nanoparticles are used in various fields of science and technology, and have been shown to be a strong counterpart to organic and organometallic phosphors [26–28] in many applications, e.g. LEDs [29,30]. They are also promising for lasers [31,32], biosensors [33,34], and photonic devices [35,36]. However, for the correct functioning of electronic

---

Received 30 July 2024; revised 8 October 2024; accepted 10 October 2024.  
Available online 30 October 2024

\* Corresponding author.

E-mail addresses: daibagya@mail.ru (D.S. Daibagya), zakharchukia@yandex.ru (I.A. Zakharchuk), s.ambrozevich@bmtu.ru (S.A. Ambrozevich), smirnov\_m\_s@mail.ru (M.S. Smirnov), anna.v.osadchenko@gmail.com (A.V. Osadchenko), ovchinnikov\_o\_v@rambler.ru (O.V. Ovchinnikov), selyukov@lebedev.ru (A.S. Selyukov).

<https://doi.org/10.33640/2405-609X.3378>

2405-609X/© 2024 University of Kerbala. This is an open access article under the CC-BY-NC-ND license (<http://creativecommons.org/licenses/by-nc-nd/4.0/>).

devices based on colloidal nanocrystals and, in particular, QDs, various factors (temperature, electric field, and temporal behaviour) should be considered and the mechanisms that lead to changes in the optical and colorimetric properties of QDs should be unveiled. To date, it has been established that changes in temperature can lead to shifts in photoluminescence (PL) spectra [37,38], which directly affects the emission color. An external electric field can lead to both enhancement [39–41] and quenching [42] of the PL intensity, as well as to the PL redshift due to the Stark effect [42]. Also, different changes in the optical properties of colloidal nanocrystals can occur over time. For example, PL photodegradation can be observed [43–45]. Effect of the environment is also a crucial problem which has been addressed in many studies. Thus, the photostability of nanocrystals has been studied in air [46], in dry air [47], in an aqueous solution [48], in nitrogen [49], in dry nitrogen [50], and in argon [50]. In these studies, photodegradation processes have been discovered. The opposite effect of photodegradation is PL intensity enhancement [51]. PL enhancement is often achieved by additional passivation of the surface of nanostructures, which can eliminate surface defects which are nonradiative recombination centers [51]. There are a number of studies reporting an increase in the emission intensity of colloidal nanostructures on a glass substrate under continuous laser irradiation in air and in nitrogen [52–54]. The shell coating contributes to the increase in the photostability and quantum yield of colloidal nanoparticles due to the effective localization of an exciton at a certain distance from the nanocrystal surface [55]. The quantum yield of colloidal nanocrystals covered with a semiconductor shell can reach 85–95% [56]. However, the shell does not always provide complete elimination of various negative effects in nanocrystals. Thus, the study of luminescence photostability for colloidal nanocrystals is an important task since the understanding of the corresponding physical processes advances the efficiency of new electronic devices based on semiconductor nanoparticles. For example, in Ref. [57], almost complete photostability of the bandgap of CdTe/SiO<sub>2</sub> QDs at elevated temperatures has been found.

In the present study, we first address the photostability of PL intensity of CdTe/SiO<sub>2</sub> QDs under continuous laser irradiation to reveal the corresponding mechanisms responsible for their emission behavior.

## 2. Materials and methods

### 2.1. Synthesis

Colloidal synthesis of the QDs is based on the use of organic ligands with a thiol group and their subsequent substitution [58]. Tellurium precursor solution was obtained by mixing 0.25 mmol of a TeO<sub>3</sub> powder and 25 ml of water in a flask at room temperature. Then, a NaBH<sub>4</sub> powder was added into the flask until a pink-colored solution was obtained. This resulted in a solution of the tellurium precursor. The cadmium precursor was a salt of cadmium and 3-mercaptopropionic acid. For its synthesis, 0.25 mmol of CdBr<sub>2</sub> was dissolved in another flask containing 50 ml of water at 30 °C. Then, 0.675 mmol of 3-mercaptopropionic acid (3-MPA) was added. The solution became milky white. After that, the pH was increased to 10 by adding 1 mol/l of NaOH. In this case, the solution became transparent, indicating the formation of the Cd/3-MPA cadmium precursor. Then, the tellurium precursor solution was mixed with the Cd/3-MPA solution with constant stirring by a magnetic stirrer rotating at 300 rpm. The temperature of the solution during mixing was 30 °C. To ensure complete reaction, the prepared mixture was kept at 30 °C for 30 min with constant stirring. To remove the reaction products, acetone was added to the colloidal solution of the CdTe/3-MPA QDs in equal quantities (5 ml of acetone was added to 5 ml of CdTe QDs). The resulting mixture was centrifuged at 5000 rpm for 15 min and re-dissolved in 5 ml of distilled water. The purification procedure was repeated 3 times. The silica shell was formed on the surface of the QDs using an aqueous synthesis. The purified CdTe/3-MPA QDs were dissolved in 250 mL of distilled water and placed in a three-necked flask. To coat the QDs with a SiO<sub>2</sub> layer, an aqueous solution of 1 mmol of 3-mercaptopropyltrimethoxysilane was added to the QD solution. 3-mercaptopropyltrimethoxysilane was preliminarily dissolved in 50 mL of distilled water at 25 °C and kept for 5 h. After adding the 3-mercaptopropyltrimethoxysilane solution to the QDs, the mixture was stirred for 2 h at 25 °C. This provided the replacement of 3-MPA with 3-mercaptopropyltrimethoxysilane at the QD interface. Thus, a SiO<sub>2</sub> monolayer was formed. To form a thicker shell, 50 mmol of sodium metasilicate was then added to the QD solution and the solution was kept under constant stirring at 300 rpm with a magnetic stirrer at 25 °C for another 2 h. The product CdTe/SiO<sub>2</sub>

QDs were purified from the reaction mixture using the method described above (precipitated with acetone and centrifuged).

## 2.2. Morphology and absorption measurements

The size distribution and morphology of the synthesized QDs were studied using a JEM-2100 transmission electron microscope (TEM; JEOL, Japan).

The absorption spectrum of the QD aqueous solution was acquired by a Lambda 45 UV/Vis spectrophotometer (Perkin-Elmer, USA) within the 200–600 nm wavelength range.

The X-ray diffraction pattern was measured within  $2\theta = 10^\circ\text{--}70^\circ$  using a DRON-4-07 diffractometer with  $\text{Cu K}\alpha$  radiation.

The FTIR spectrum was obtained with an FSM 2202 instrument operating within the  $370\text{--}7800\text{ cm}^{-1}$  range at room temperature using a KBr substrate.

## 2.3. PL measurements

PL spectra were recorded at room temperature for QDs drop casted on a glass substrate using the Ocean Optics Maya Pro 2000 spectrometer with an LDH-C 400 pulsed laser (PicoQuant, Germany) used for excitation. The laser emission wavelength was 405 nm, the pulse duration was 75 ps, the average emission power was 5 mW, and the repetition rate was 40 MHz.

The PL quantum yield was measured by a relative method at room temperature using Coumarin 153 in ethanol as the standard [59].

## 3. Results and discussion

### 3.1. Morphology studies

The TEM image of the synthesized colloidal CdTe/SiO<sub>2</sub> QDs is presented in Fig. 1a. It can be seen that the nanocrystals have a spherical shape. The size distribution of the nanocrystals is given in

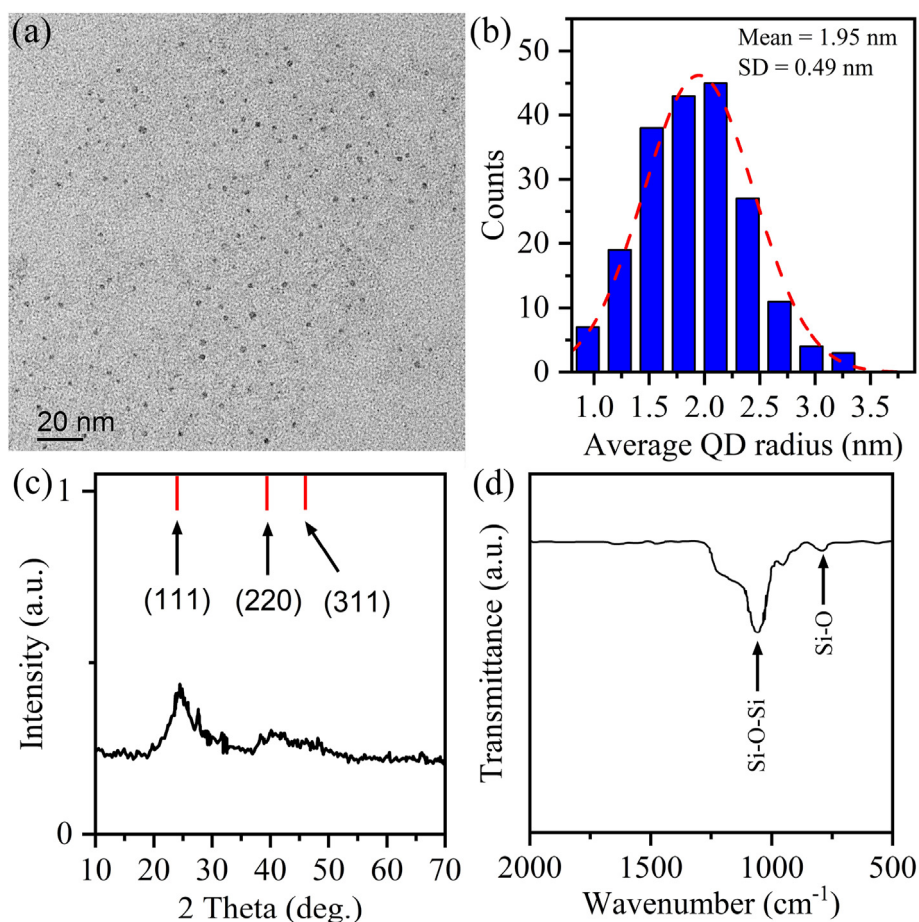


Fig. 1. (a) TEM-image of the synthesized colloidal semiconductor CdTe/SiO<sub>2</sub> QDs; (b) The size distribution of the synthesized QDs. The dashed curve is a Gaussian fit to the data; (c) XRD pattern for the CdTe/SiO<sub>2</sub> QDs; (d) FTIR spectrum the CdTe/SiO<sub>2</sub> QDs.

**Fig. 1b.** The dashed red curve is a Gaussian function  $a \cdot \exp(-(R - \text{Mean})^2 / 2 \cdot \text{SD}^2)$ . Here  $a$  is the amplitude,  $R$  is the radius of the QDs,  $\text{Mean}$  is the average radius of the QDs, and  $\text{SD}$  is the standard deviation. The average radius of the colloidal CdTe/SiO<sub>2</sub> QDs was obtained to be 1.95 nm with  $\text{SD} = 0.49$  nm. The XRD pattern shown in Fig. 1c was used to determine the phase structure of CdTe/SiO<sub>2</sub> QDs. The diffraction features at 24.03°, 39.47°, and 46.48° are due to the (111), (220), and (311) crystal planes and are attributed to the cubic CdTe (JCPDS Card No. 15–0770). The weak intensity of the diffraction peaks is due to the presence of the SiO<sub>2</sub> shell. Also, a FTIR analysis has been conducted (Fig. 1d). Bands at 1060 and 790 cm<sup>-1</sup> were observed, which can be attributed to asymmetric Si-O-Si stretching vibrations and symmetric Si-O stretching vibrations specific to CdTe/SiO<sub>2</sub> core/shell systems [60,61].

### 3.2. Optical properties

The samples were studied by absorption and emission spectroscopies (Fig. 2a). The absorption band with a maximum at ~456 nm (Fig. 2a, blue curve) is associated with electronic transitions between the valence band and the conduction band of the QDs [62]. In the PL spectrum (Fig. 2a, red curve) of the CdTe/SiO<sub>2</sub> QDs, a band due to the interband

transition is observed. The PL intensity maximum is at 521 nm, and the full width at half-maximum (FWHM) of the PL spectrum is 56 nm. At longer wavelengths, a noticeable broadening of the PL band is observed in the wing of the spectrum, which may be due to the very weak trap-state luminescence [63]. The quantum yield of the CdTe/SiO<sub>2</sub> QDs was measured to be 42%.

Using the wavelength (456 nm) of the first exciton peak in the absorption spectrum, we can estimate the average size of the QDs using the following relation [64]:

$$E_g^{\text{QD}} = E_g^{\text{Bulk}} + \frac{h^2}{8R^2} \left[ \frac{1}{m_e} + \frac{1}{m_h} \right] - \frac{1.8e^2}{4\pi\epsilon\epsilon_0R}$$

Here  $E_g^{\text{QD}}$  is the QD bandgap,  $E_g^{\text{Bulk}}$  (1.475 eV [65]) is the bandgap of the bulk CdTe crystal,  $h$  is the Planck's constant,  $e$  is the elementary charge,  $m_e = 0.11m_0$  and  $m_h = 0.35m_0$  [65] are the effective masses of electrons and holes, respectively,  $m_0$  is the electron rest mass,  $\epsilon_0$  is the electric constant,  $\epsilon = 7.1$  [64] is the dielectric constant of the CdTe QDs, and  $R$  is the average radius of the CdTe QDs. According to the calculations, the average radius of the QDs under study is 1.76 nm. The maxima of the absorption and PL spectra of the colloidal CdTe/SiO<sub>2</sub> QDs are shifted to the blue region relative to thicker

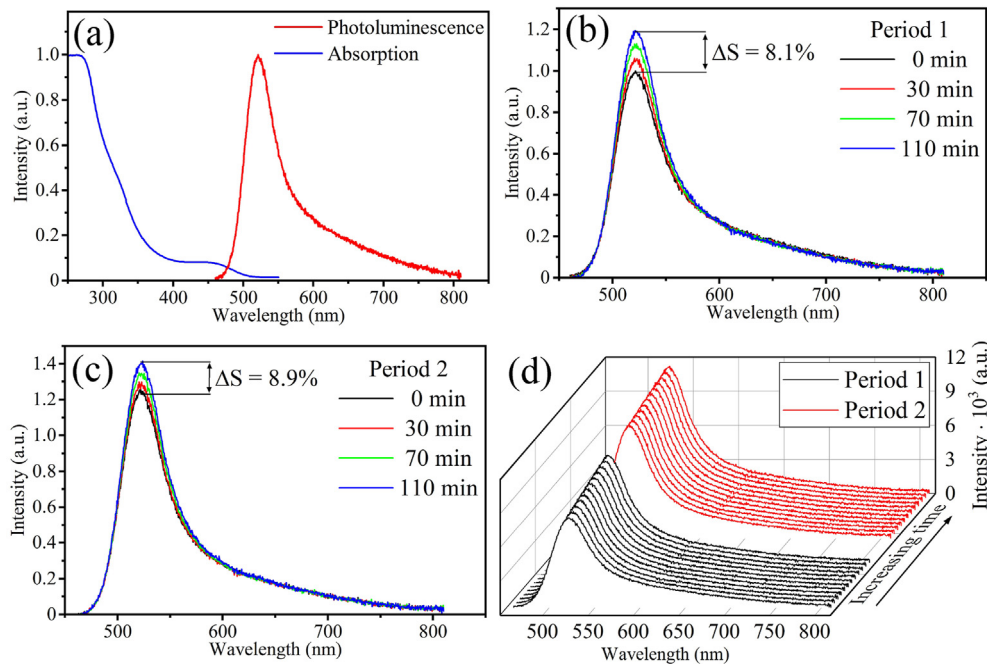


**Fig. 2.** (a) Absorption (blue curve) and PL (red curve) spectra of the CdTe/SiO<sub>2</sub> QDs at room temperature; (b) PL spectra of the CdTe/SiO<sub>2</sub> QDs obtained under continuous laser irradiation for “Period 1”; (c) PL spectra of the CdTe/SiO<sub>2</sub> QDs obtained under continuous laser irradiation for “Period 2”; (d) Representative series of PL spectra for “Period 1” and “Period 2”. PL spectra for “Period 2” are normalized relative to the first spectrum obtained for “Period 1”.

CdTe QDs and bulk CdTe crystal, which is due to the quantum confinement effect [64,66,67].

### 3.3. PL intensity enhancement

To measure the time dependence of the PL intensity of the CdTe/SiO<sub>2</sub> QDs under continuous laser irradiation, PL spectra were recorded every 10 min for 110 min. Then, the laser was switched off for 1 h and then turned on again for 110 min with the PL spectra registered every 10 min. The experiment carried out before the laser was turned off will be called “Period 1” and the experiment carried out after the laser was turned on again will be referred to as “Period 2”. To quantify the observed effects, the integrated PL intensity was calculated using the following relation:

$$S = \int_{\lambda_1}^{\lambda_2} I(\lambda) d\lambda.$$

Here  $S$  is the integrated PL intensity for the CdTe/SiO<sub>2</sub> QDs,  $I(\lambda)$  is the PL intensity as a function of wavelength, the integration limits are  $\lambda_1 = 460$  nm and  $\lambda_2 = 810$  nm.

The PL spectra of the CdTe/SiO<sub>2</sub> QDs at different time points recorded under continuous laser irradiation during “Period 1” are shown in Fig. 2b. It can be seen that the PL intensity increases with time, while the shape of the spectrum does not change significantly. For “Period 1”, the integrated PL intensity increased by ~8.1%. After recording the spectra for “Period 1”, the laser radiation was switched off for 1 h.

The PL spectra of the colloidal CdTe/SiO<sub>2</sub> nanocrystals at different time points recorded under continuous laser irradiation during “Period 2” are shown in Fig. 2c. These spectra are normalized relative to the first spectrum recorded for “Period 1” (Fig. 2b, black curve). It can be seen that the PL intensity is also increased for “Period 2”. The shape of the spectra did not change significantly. The integrated PL intensity increased by about 8.9%. A representative series of PL spectra for “Period 1” and “Period 2” is shown in Fig. 2d.

The integrated PL intensity for the colloidal semiconductor CdTe/SiO<sub>2</sub> QDs continuously increases with time (Fig. 3a). The integrated PL intensity increased by about 22% over the entire experimental time range (Fig. 3b). The enhancement of the luminescence intensity can be related to the adsorption of water molecules on the surface of the QDs [49,51,52]. Consequently, passivation of defect states occurs, and thus a number of “dark” QDs

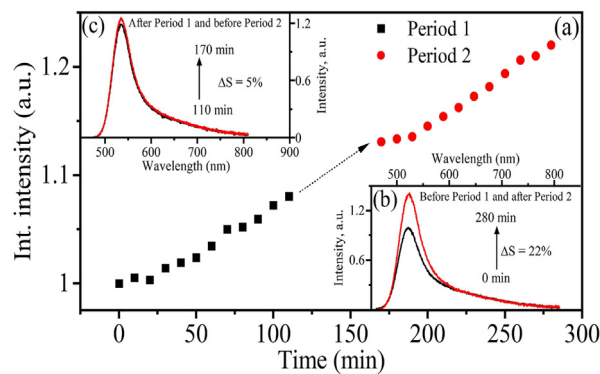


Fig. 3. (a) Time dependence of the integrated PL intensity for the CdTe/SiO<sub>2</sub> QDs; (b) PL spectra before “Period 1” (black curve) and after “Period 2” (red curve); (c) PL spectra after “Period 1” (black curve) and before “Period 2” (red curve).

[49,51] turn into “bright” QDs. In other words, the probability of nonradiative transitions in the QD ensemble decreases due to the trap passivation. Notably, in Ref. [51] core-only CdTe QDs have been studied under continuous laser irradiation and similar intensity enhancement has been observed. However, after approximately 200 min of irradiation, it turned into intensity quenching with a significant blueshift due to photocorrosion. None of the latter effects are observed in our case due to the protective effect of the SiO<sub>2</sub> shell, which will be discussed below. Moreover, after a 60 min “break” in the irradiation, the integrated PL intensity increased by ~5% (Fig. 3c) in contrast to the expected decrease [49]. The observed increase in the PL intensity after keeping the QDs in the dark suggests that the trap passivation process continues even in the absence of irradiation.

During the entire time of the experiment (“Period 1” + “Period 2”), the position of the PL intensity maximum for the colloidal CdTe/SiO<sub>2</sub> QDs is almost unchanged (Fig. 4a). This can be explained by the fact that for the CdTe core capped with a large-bandgap (~8.9 eV [68]) inorganic SiO<sub>2</sub> shell, photocorrosion, which is often responsible for the PL blueshift, is a slow process [52,53].

The color coordinates ( $x$ ;  $y$ ) calculated in the CIE 1931 space, dominant wavelength  $\lambda^*$ , color purity (CP), and correlated color temperature  $T_c$  for the investigated QDs are presented in Table 1 [69–71]. The color coordinates obtained for the PL of the CdTe/SiO<sub>2</sub> nanocrystals are almost at the edge of the chromaticity diagram (Fig. 4b) in the green region, indicating a high color purity (CP = 81%). The dominant wavelength is  $\lambda^* = 556$  nm. As a result of the luminescence intensity enhancement for 280 min, the color coordinates are slightly shifted to the blue region. At the same time, the color purity of

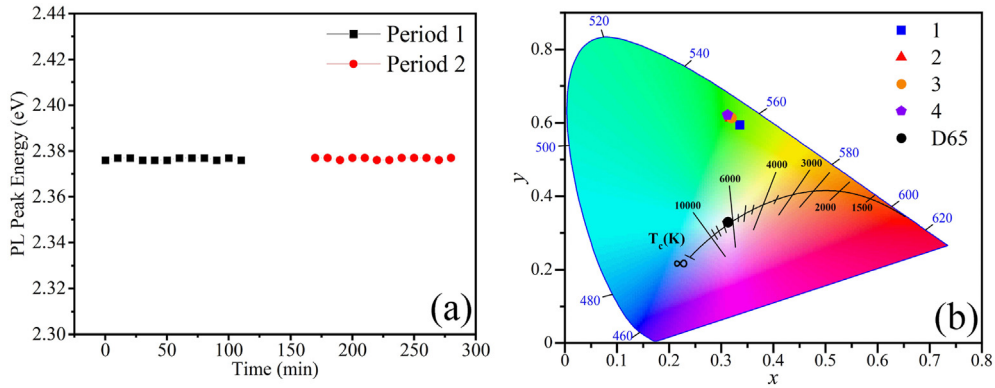


Fig. 4. (a) Time dependence of the PL intensity maximum for the CdTe/SiO<sub>2</sub> QDs under continuous laser irradiation; (b) Chromaticity diagram: 1 is PL of the QDs before “Period 1”; 2 is PL of the QDs after “Period 1”; 3 is PL of the QDs before “Period 2”; 4 is PL of the QDs after “Period 2”; D65 is the standard radiation (white light); solid black line is the Planck’s curve; T<sub>c</sub> (K) is the correlated color temperature.

Table 1. Color coordinates, dominant wavelength, color purity, and correlated color temperature for CdTe/SiO<sub>2</sub> QD emission.

Time	Color coordinates		λ* (nm)	CP (%)	T <sub>c</sub> (K)
	x	y			
1 – Before “Period 1”	0.336	0.594	556	81	5457
2 – After “Period 1”	0.319	0.613	553	83	5737
3 – Before “Period 2”	0.340	0.613	553	83	5716
4 – After “Period 2”	0.312	0.621	551	84	5837

the investigated QDs is increased by 3%. Hence, it is potentially possible to obtain PL with higher color purity at prolonged irradiation.

### 3.4. PL intensity enhancement mechanism

Let us consider the mechanisms of the PL intensity enhancement for the colloidal CdTe/SiO<sub>2</sub>

semiconductor QDs (Fig. 5). The studied samples consist of an ensemble of QDs. At the initial moment of time (Fig. 5a), electrons (e<sub>1</sub> and e<sub>2</sub>) in the ensemble of the QDs are excited (black solid arrow) under continuous laser irradiation, which can further relax from the conduction band to the valence band both radiatively (red arrow) and nonradiatively (black dashed arrow) through the

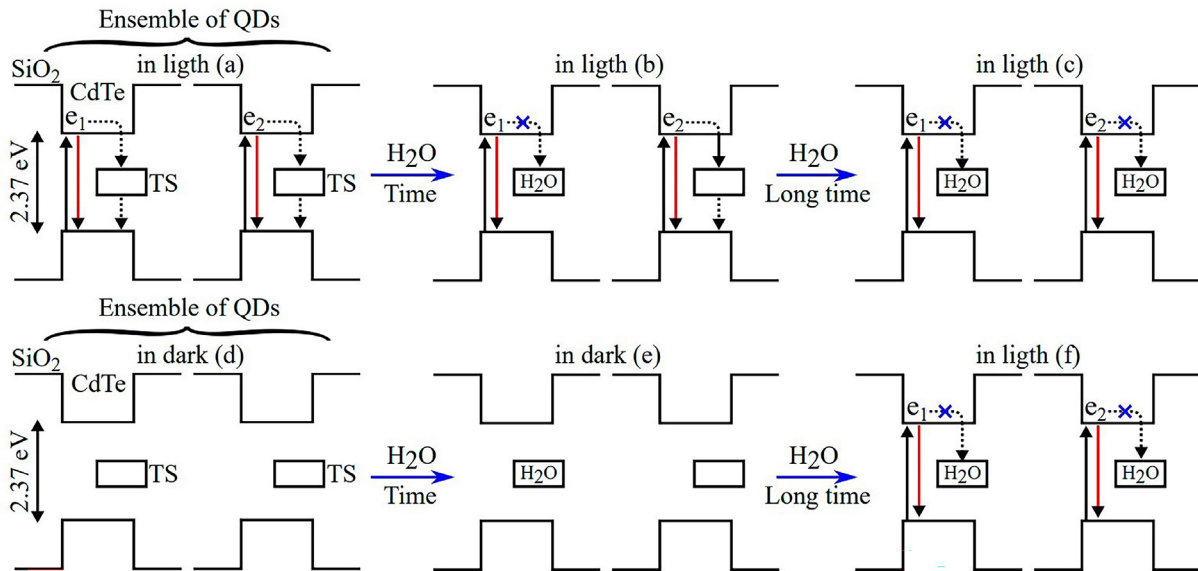


Fig. 5. Mechanism of the PL intensity enhancement for the CdTe/SiO<sub>2</sub> QDs under continuous laser irradiation (top) and without it (bottom): (a) Initial time point under continuous laser irradiation; (b) Some time after the start of irradiation; (c) Long time after the start of irradiation; (d) Initial time point in the absence of laser irradiation; (e) Some time after the beginning of the experimental phase when optical radiation is absent; (f) Moment of switching on the excitation radiation again.



trap state (TS). Water molecules are then adsorbed on the surface of several QDs and passivate the surface traps (Fig. 5b), thereby reducing the probability of nonradiative transitions and, consequently, increasing the QD PL intensity [49,51,52]. Eventually, the number of QDs with passivated traps increases in the ensemble (Fig. 5c). Thus, the number of radiative transitions increases, which results in an increase in the amplitude of the PL maximum (Fig. 2b–d) and integrated PL intensity (Fig. 3) under continuous laser irradiation. Let us now consider the possible mechanism of PL enhancement for the sample kept in the dark after irradiation. Let us assume that no transitions occur in the absence of laser radiation (Fig. 5d). In fact, spontaneous nonradiative transitions are possible both between the valence and conduction bands and through trap levels, but in our case such transitions do not contribute to the PL intensity. Therefore, they are absent in Fig. 5d. It is assumed that in the dark, the process of adsorption of water molecules on the surface of QDs does not stop and the passivation of traps continues (Fig. 5e). Thus, the number of QDs with passivated traps after storing them in the dark appears to be greater than the number of QDs with passivated defects at the beginning of the experimental phase when the laser is switched off. In other words, the probability of radiative transitions after storing the QDs in the dark before the second irradiation period is greater than that at the beginning of the experiment when radiation is absent. That is why, when the excitation radiation is switched on (Fig. 5f) after the QDs have been stored in the dark, the increase in the PL intensity (Fig. 3c) and the integrated PL intensity (Fig. 3a) with respect to the last spectrum registered for “Period 1” is observed.

#### 4. Conclusions

In summary, the present study concerns the luminescent properties of colloidal CdTe/SiO<sub>2</sub> core/shell QDs under continuous laser irradiation at room temperature. It is revealed that PL of the investigated nanostructures is due to both interband and trap-state transitions. It is found that under continuous laser irradiation, there is an increase in the PL intensity for the QDs in time. The observed luminescence intensity enhancement is associated with adsorption of water molecules on the surface of the QDs and the resulting decrease in the probability of nonradiative transitions. The absence of the displacement of the PL intensity maximum can be explained by the fact that for the CdTe core capped with a large-bandgap inorganic SiO<sub>2</sub> shell, photocorrosion, which is often responsible for the PL

blueshift, is a slow process. It is shown that the color purity of the PL increased for 280 min by 3% due to the discussed effects. The results of our work can be used in the development of optoelectronic and nanophotonic devices based on colloidal semiconductor CdTe/SiO<sub>2</sub> nanostructures. Moreover, the demonstrated stability of the PL peak position makes the studied QDs promising for biological marker application.

#### Disclosure statement

The authors report there are no competing interests to declare.

#### Funding

This work was supported by the Ministry of Science and Higher Education of Russia under Agreement No. 075-15-2021-1351 in part of the structural analysis of colloidal QDs.

#### Ethics information

This research is not related to ethical issues as it does not involve living organisms.

#### Acknowledgements

Authors are very grateful to N. Tabachkova (Prokhorov General Physics Institute of the Russian Academy of Sciences) for TEM studies of the QDs.

#### References

- [1] P. Zhang, Y. Wang, X. Su, Q. Zhang, M. Sun, Study of laser-induced multi-exciton generation and dynamics by multiphoton absorption in CdSe quantum dots, *Nanomaterials* 14 (2024) 558–668, <https://doi.org/10.3390/nano14070558>.
- [2] I. Grevtseva, O. Ovchinnikov, M. Smirnov, A. Perepelitsa, T. Chevychelova, V. Derepko, A. Osadchenko, A. Selyukov, IR luminescence of plexcitonic structures based on Ag<sub>2</sub>S/L-Cys quantum dots and Au nanorods, *Opt. Express*. 30 (2022) 4668–4679, <https://doi.org/10.1364/OE.447200>.
- [3] D.S. Daibagya, S.A. Ambrozevich, A.S. Perepelitsa, I.A. Zakharchuk, A.V. Osadchenko, D.M. Bezverkhnyaya, A.I. Avramenko, A.S. Selyukov, Spectral and kinetic properties of silver sulfide quantum dots in an external electric field, *Sci. Tech. J. Inf. Technol. Mech. Opt.* 146 (2022) 1098–1103, <https://doi.org/10.17586/2226-1494-2022-22-6-1098-1103>.
- [4] Y.B. Chae, S.Y. Kim, H.D. Choi, D.G. Moon, K.H. Lee, C.K. Kim, Enhancing efficiency in Inverted quantum dot light-emitting diodes through arginine-modified ZnO nanoparticle electron injection layer, *Nanomaterials* 14 (2024) 266–284, <https://doi.org/10.3390/nano14030266>.
- [5] K. Tosa, C. Ding, S. Chen, S. Hayase, Q. Shen, Classifying the role of surface ligands on the passivation and stability of Cs<sub>2</sub>NaInCl<sub>6</sub> double perovskite quantum dots, *Nanomaterials* 14 (2024) 376–388, <https://doi.org/10.3390/nano14040376>.
- [6] V.N. Derepko, O.V. Ovchinnikov, M.S. Smirnov, I.G. Grevtseva, T.S. Kondratenko, A.S. Selyukov, S.Y. Turishchev, Plasmon-exciton nanostructures, based on CdS quantum

- dots with exciton and trap state luminescence, *J. Lumin.* 248 (2022) 118874, <https://doi.org/10.1016/j.jlumin.2022.118874>.
- [7] N.N. Jawhar, E. Soheyli, A.F. Yazici, E. Mutlugun, R. Sahraei, Preparation of highly emissive and reproducible Cu–In–S/ZnS core/shell quantum dots with a mid-gap emission character, *J. Alloys Compd.* 824 (2020) 153906, <https://doi.org/10.1016/j.jallcom.2020.153906>.
- [8] Z. Seidalilir, S. Shishehbor, E. Soheyli, M. Sabaeian, Impact of red emissive ZnCdTeS quantum dots on the electro-optic switching, dielectric and electrochemical features of nematic liquid crystal: towards tunable optoelectronic systems, *Opt. Mater.* 140 (2023) 113868, <https://doi.org/10.1016/j.optmat.2023.113868>.
- [9] M. Kaladzian, N. von den Driesch, N. Demarina, I. Povstugar, E. Zimmermann, M.M. Jansen, J.H. Bae, C. Krause, B. Bennemann, D. Grützmacher, T. Schäpers, Growth and electrical characterization of hybrid core/shell InAs/CdSe nanowires, *ACS Appl. Mater. Interfaces.* 16 (2024) 11035–11042, <https://doi.org/10.1021/acsami.3c18267>.
- [10] N. Bastami, E. Soheyli, A. Arslan, R. Sahraei, A.F. Yazici, E. Mutlugun, Nanowire-shaped MoS<sub>2</sub>@MoO<sub>3</sub> nanocomposites as a hole injection layer for quantum dot light-emitting diodes, *ACS Appl. Electron. Mater.* 4 (2022) 3849–3859, <https://doi.org/10.1021/acsaem.2c00485>.
- [11] J. He, H. Li, C. Liu, X. Wang, Q. Zhang, J. Liu, M. Wang, Y. Liu, Hot-Injection synthesis of cesium lead halide perovskite nanowires with tunable optical properties, *Materials* 17 (2024) 2173–2184, <https://doi.org/10.3390/ma17102173>.
- [12] A.G. Vitukhnovskiy, A.S. Selyukov, V.R. Solovey, R.B. Vasiliev, E.P. Lazareva, Photoluminescence of CdTe colloidal quantum wells in external electric field, *J. Lumin.* 186 (2017) 194–198, <https://doi.org/10.1016/j.jlumin.2017.02.041>.
- [13] Z. Ouzit, G. Baillard, J. Liu, B. Wagnon, L. Guillemeney, B. Abécassis, L. Coolen, Luminescence dynamics of single self-assembled chains of Förster (FRET)-Coupled CdSe nanoplatelets, *J. Phys. Chem. Lett.* 14 (2023) 6209–6216, <https://doi.org/10.1021/acs.jpcclett.3c00908>.
- [14] A.A. Vashchenko, A.G. Vitukhnovskii, V.S. Lebedev, A.S. Selyukov, R.B. Vasiliev, M.S. Sokolikova, Organic light-emitting diode with an emitter based on a planar layer of CdSe semiconductor nanoplatelets, *JETP Lett* 100 (2014) 86–90, <https://doi.org/10.1134/S0021364014140124>.
- [15] S.R. Meliakov, V.V. Belykh, I.V. Kalitukha, A.A. Golovatenko, A. Di Giacomo, I. Moreels, A.V. Rodina, D.R. Yakovlev, Coherent spin dynamics of electrons in CdSe colloidal nanoplatelets, *Nanomaterials* 13 (2023) 3077–3092, <https://doi.org/10.3390/nano13233077>.
- [16] A.A. Babaev, I.D. Skurlov, S.A. Cherevko, P.S. Parfenov, M. A. Baranov, N.K. Kuzmenko, A.V. Koroleva, E.V. Zhizhin, A. V. Fedorov, PbSe/PbS core/shell nanoplatelets with enhanced stability and photoelectric properties, *Nanomaterials* 13 (2023) 3051–3061, <https://doi.org/10.3390/nano13233051>.
- [17] C. Bouet, B. Mahler, B. Nadal, B. Abecassis, M.D. Tessier, S. Ithurria, X. Xu, B. Dubertret, Two-dimensional growth of CdSe nanocrystals, from nanoplatelets to nanosheets, *Chem. Mater.* 25 (2013) 639–645, <https://doi.org/10.1021/cm304080q>.
- [18] D.S. Daibagya, I.A. Zakharchuk, A.V. Osadchenko, A.S. Selyukov, S.A. Ambrozevich, M.L. Skorikov, R.B. Vasiliev, Luminescence and colorimetric properties of ultrathin cadmium selenide nanoscrolls, *Bull. Lebedev Phys. Inst.* 50 (2023) 510–514, <https://doi.org/10.3103/S1068335623110118>.
- [19] A.I. Zvyagin, T.A. Chevychelova, K.S. Chirkov, M.S. Smirnov, O.V. Ovchinnikov, A.S. Selyukov, A.N. Latyshev, Enhancement of nonlinear absorption of nanosecond laser pulses in mixtures of Ag<sub>2</sub>S quantum dots and silver nanoparticles, *Bull. Lebedev Phys. Inst.* 50 (2023) 1532–1535, <https://doi.org/10.3103/S1068335623602121>.
- [20] O. Korepanov, D. Kozodaev, O. Aleksandrova, A. Bugrov, D. Firsov, D. Kirilenko, D. Mazing, V. Moshnikov, Z. Shomakhov, Temperature- and size-dependent photoluminescence of CuInS<sub>2</sub> quantum dots, *Nanomaterials* 13 (2023) 2892–3904, <https://doi.org/10.3390/nano13212892>.
- [21] I.G. Grevtseva, O.V. Ovchinnikov, M.S. Smirnov, A.S. Perpelitsa, T.A. Chevychelova, V.N. Derepko, A.V. Osadchenko, A.S. Selyukov, The structural and luminescence properties of plexcitonic structures based on Ag<sub>2</sub>S/I-Cys quantum dots and Au nanorods, *RSC Adv* 12 (2022) 6525–6532, <https://doi.org/10.1039/D1RA08806H>.
- [22] W. Guo, X. Song, J. Liu, W. Liu, X. Chu, Z. Lei, Quantum dots as a potential multifunctional material for the enhancement of clinical diagnosis strategies and cancer treatments, *Nanomaterials* 14 (2024) 1088–1113, <https://doi.org/10.3390/nano14131088>.
- [23] A.I. Zvyagin, T.A. Chevychelova, I.G. Grevtseva, M.S. Smirnov, A.S. Selyukov, O.V. Ovchinnikov, R.A. Ganeev, Nonlinear refraction in colloidal silver sulfide quantum dots, *J. Russ. Laser Res.* 41 (2020) 670–680, <https://doi.org/10.1007/s10946-020-09923-4>.
- [24] N.V. Korolev, M.S. Smirnov, O.V. Ovchinnikov, T.S. Shatskikh, Energy structure and absorption spectra of colloidal CdS nanocrystals in gelatin matrix, *Phys. E: Low-Dimens. Syst. Nanostructures.* 68 (2015) 159–163, <https://doi.org/10.1016/j.physe.2014.10.042>.
- [25] J. Liu, Y. Nie, W. Xue, L. Wu, H. Jin, G. Jin, Z. Zhai, C. Fu, Size effects on structural and optical properties of tin oxide quantum dots with enhanced quantum confinement, *J. Mater. Res. Technol.* 9 (2020) 8020–8028, <https://doi.org/10.1016/j.jmrt.2020.05.041>.
- [26] Z. Lin, S. Gao, S. Wang, J.Y. Wu, Regulation and application of organic luminescence from low-dimensional organic-inorganic hybrid metal halides, *J. Mater. Chem. C.* 11 (2023) 16890–16911, <https://doi.org/10.1039/D3TC03772J>.
- [27] A.V. Osadchenko, A.A. Vashchenko, I.A. Zakharchuk, D.S. Daibagya, S.A. Ambrozevich, N.Yu Volodin, D.A. Cheptsov, S.M. Dolotov, V.F. Traven, A.I. Avramenko, S.L. Semenova, A.S. Selyukov, Organic light-emitting diodes with new dyes based on coumarin, *Sci. Tech. J. Inf. Technol. Mech. Opt.* 22 (2022) 1112–1118, <https://doi.org/10.17586/2226-1494-2022-22-6-1112-1118>.
- [28] J. Luo, X.F. Rong, Y.Y. Ye, W.Z. Li, X.Q. Wang, W. Wang, Research progress on triarylmethyl radical-based high-efficiency OLED, *Molecules* 27 (2022) 1632–1653, <https://doi.org/10.3390/molecules27051632>.
- [29] D. Bozyigit, O. Yarema, V. Wood, Origins of low quantum efficiencies in quantum dot LEDs, *Adv. Funct. Mater.* 23 (2013) 3024–3029, <https://doi.org/10.1002/adfm.201203191>.
- [30] A.S. Selyukov, A.G. Vitukhnovskii, V.S. Lebedev, A.A. Vashchenko, R.B. Vasiliev, M.S. Sokolikova, Electroluminescence of colloidal quasi-two-dimensional semiconducting CdSe nanostructures in a hybrid light-emitting diode, *J. Exp. Theor. Phys.* 120 (2015) 595–606, <https://doi.org/10.1134/S1063776115040238>.
- [31] X. Su, Y. Pan, D. Gao, J. Wang, H. Yu, R. Chen, B. Guan, X. Yang, Y. Wang, L. Wang, Surface vertical multi-emission laser with distributed Bragg reflector feedback from CsPbI<sub>3</sub> quantum dots, *Nanomaterials* 13 (2023) 1669–1680, <https://doi.org/10.3390/nano13101669>.
- [32] Y. Gu, Z. Yang, Z. Li, Field manipulations in on-chip micro/nanoscale lasers based on colloid nanocrystals, *Nanomaterials* 13 (2023) 3069–3090, <https://doi.org/10.3390/nano13233069>.
- [33] Y. Tao, Y. Zhao, L. Wang, J. Huang, Y. Chen, Q. Huang, B. Song, H.Y. Li, J. Chen, H. Liu, Flexible amperometric immunosensor based on colloidal quantum dots for detecting the myeloperoxidase (MPO) systemic inflammation biomarker, *Biosensors* 13 (2023) 255–264, <https://doi.org/10.3390/bios13020255>.
- [34] E. Soheyli, B. Ghaemi, R. Sahraei, Z. Sabzevari, S. Kharrazi, A. Amani, Colloidal synthesis of tunably luminescent AgInS-based/ZnS core/shell quantum dots as biocompatible nanoprobe for high-contrast fluorescence bioimaging, *Mater. Sci. Eng. C.* 111 (2020) 110807, <https://doi.org/10.1016/j.msec.2020.110807>.
- [35] M. Chen, L. Lu, H. Yu, C. Li, N. Zhao, Integration of colloidal quantum dots with photonic structures for optoelectronic

- and optical devices, *Adv. Sci.* 8 (2021) 2101560, <https://doi.org/10.1002/advs.202101560>.
- [36] J. Kim, S. Song, Y.H. Kim, S.K. Park, Recent progress of quantum dot-based photonic devices and systems: a comprehensive review of materials, devices, and applications, *Small Struct* 2 (2021) 2000024, <https://doi.org/10.1002/sstr.202000024>.
- [37] S.F. Wuister, C. de Mello Donegá, A. Meijerink, Luminescence temperature anti-quenching of water-soluble CdTe quantum dots: role of the solvent, *J. Am. Chem. Soc.* 126 (2004) 10397–10402, <https://doi.org/10.1021/ja048222a>.
- [38] H. Wu, W. Zhang, K. Li, C. Liu, Optical properties of CdTe quantum dots in silicate glasses containing CaO, *Opt. Mater.* 148 (2024) 114897, <https://doi.org/10.1016/j.optmat.2024.114897>.
- [39] B.W. Garner, T. Cai, Z. Hu, A. Neogi, Electric field enhanced photoluminescence of CdTe quantum dots encapsulated in poly (N-isopropylacrylamide) nano-spheres, *Opt. Express.* 16 (2008) 19410–19418, <https://doi.org/10.1364/OE.16.019410>.
- [40] Z. Wang, Z. Huang, G. Liu, B. Cai, S. Zhang, Y. Wang, In-situ and reversible enhancement of photoluminescence from CsPbBr<sub>3</sub> nanoplatelets by electrical bias, *Adv. Opt. Mater.* 9 (2021) 2100346, <https://doi.org/10.1002/adom.202100346>.
- [41] D.S. Daibagya, S.A. Ambrozevich, A.S. Perepelitsa, I.A. Zakharchuk, M.S. Smirnov, O.V. Ovchinnikov, S.V. Aslanov, A.V. Osadchenko, A.S. Selyukov, Electric field influence on the recombination luminescence of the colloidal silver sulfide quantum dots, *Her. Bauman Moscow State Tech. Univ. Ser. Nat. Sci.* 3 (2023) 100–117, <https://doi.org/10.18698/1812-3368-2023-3-100-117>.
- [42] H. Asif, R. Sahin, Stark control of plexcitonic states in incoherent quantum systems, *Phys. Rev. A* 110 (2024) 023713, <https://doi.org/10.1103/PhysRevA.110.023713>.
- [43] R. An, F. Zhang, X. Zou, Y. Tang, M. Liang, I. Oshchepovskyy, Y. Liu, A. Honarfar, Y. Zhong, C. Li, H. Geng, Photostability and photodegradation processes in colloidal CsPbI<sub>3</sub> perovskite quantum dots, *ACS Appl. Mater. Interfaces.* 10 (2018) 39222–39227, <https://doi.org/10.1021/acsami.8b14480>.
- [44] O.V. Ovchinnikov, I.G. Grevtseva, M.S. Smirnov, T.S. Konratenko, Reverse photodegradation of infrared luminescence of colloidal Ag<sub>2</sub>S quantum dots, *J. Lumin.* 207 (2019) 626–632, <https://doi.org/10.1016/j.jlumin.2018.12.019>.
- [45] K. Tvrđy, P.V. Kamat, Substrate-driven photochemistry of CdSe quantum dot films: charge injection and irreversible transformations on oxide surfaces, *J. Phys. Chem. A* 113 (2009) 3765–3772, <https://doi.org/10.1021/jp808562x>.
- [46] I.P. Malashin, D.S. Daibagya, V.S. Tynchenko, V.A. Nelyub, A.S. Borodulin, A.P. Gantimurov, S.A. Ambrozevich, S.A. Selyukov, ML-based forecasting of temporal dynamics in luminescence spectra of Ag<sub>2</sub>S colloidal quantum dots, *IEEE Access* 12 (2024) 53320–53334, <https://doi.org/10.1109/ACCESS.2024.3387024>.
- [47] A.A. Bol, A. Meijerink, Luminescence quantum efficiency of nanocrystalline ZnS: Mn<sup>2+</sup>. 1. Surface passivation and Mn<sup>2+</sup> concentration, *J. Phys. Chem. B* 105 (2001) 10197–10202, <https://doi.org/10.1021/jp0107560>.
- [48] H. Peng, L. Zhang, C. Soeller, J. Travas-Sejdic, Preparation of water-soluble CdTe/CdS core/shell quantum dots with enhanced photostability, *J. Lumin.* 127 (2007) 721–726, <https://doi.org/10.1016/j.jlumin.2007.04.007>.
- [49] M. Jones, J. Nedeljkovic, R.J. Ellingson, A.J. Nozik, G. Rumbles, Photoenhancement of luminescence in colloidal CdSe quantum dot solutions, *J. Phys. Chem. B* 107 (2003) 11346–11352, <https://doi.org/10.1021/jp035598m>.
- [50] J.J. Peterson, T.D. Krauss, Photobrightening and photodarkening in PbS quantum dots, *Phys. Chem. Chem. Phys.* 8 (2006) 3851–3856, <https://doi.org/10.1039/B604743B>.
- [51] S. Patra, A. Samanta, Effect of capping agent and medium on light-induced variation of the luminescence properties of CdTe quantum dots: a study based on fluorescence correlation spectroscopy, steady state and time-resolved fluorescence techniques, *J. Phys. Chem. C* 118 (2014) 18187–18196, <https://doi.org/10.1021/jp5048216>.
- [52] M.S. Zaini, J. Ying Chyi Liew, S.A. Alang Ahmad, A.R. Mohamad, M.A. Kamarudin, Quantum confinement effect and photoenhancement of photoluminescence of PbS and PbS/MnS quantum dots, *Appl. Sci.* 10 (2020) 6282–6291, <https://doi.org/10.3390/app10186282>.
- [53] Y. Wang, Z. Tang, M.A. Correa-Duarte, I. Pastoriza-Santos, M. Giersig, N.A. Kotov, L.M. Liz-Marzán, Mechanism of strong luminescence photoactivation of citrate-stabilized water-soluble nanoparticles with CdSe cores, *J. Phys. Chem. B* 108 (2004) 15461–15469, <https://doi.org/10.1021/jp048948t>.
- [54] M.V. Llopis, J.C.C. Rodriguez, F.J.F. Martín, A.M. Coto, M.T. Fernandez-Argueles, J.M. Costa-Fernández, A. Sanz-Medel, Dynamic analysis of the photoenhancement process of colloidal quantum dots with different surface modifications, *Nanotechnology* 22 (2011) 385703, <https://doi.org/10.1088/0957-4484/22/38/385703>.
- [55] C. Weisbuch, B. Vinter, *Quantum Semiconductor Structures: Fundamentals and Applications*, Academic Press, Boston, 1991.
- [56] H.S. Shim, M. Ko, S. Nam, J.H. Oh, S. Jeong, Y. Yang, S.M. Park, Y.R. Do, J.K. Song, InP/ZnSeS/ZnS quantum dots with high quantum yield and color purity for display devices, *ACS Appl. Nano Mater.* 6 (2023) 1285–1294, <https://doi.org/10.1021/acsnano.2c04936>.
- [57] S. Leviceh, A. Chahboun, A.G. Rolo, O. Conde, M.J.M. Gomes, Thermal stability of energy-emission from CdTe nanocrystals embedded in SiO<sub>2</sub> thin films, *Mod. Phys. Lett. B* 24 (2010) 2837–2843, <https://doi.org/10.1142/S0217984910025206>.
- [58] D.S. Daibagya, S.A. Ambrozevich, I.A. Zakharchuk, A.V. Osadchenko, M.S. Smirnov, O.V. Ovchinnikov, A.S. Selyukov, Emission behaviour of CdTe/SiO<sub>2</sub> core/shell quantum dots in external electric field, *Opt. Mater.* 150 (2024) 115297, <https://doi.org/10.1016/j.optmat.2024.115297>.
- [59] E. Soheyl, S. Zargoush, A.F. Yazici, R. Sahraei, E. Mutlugun, Highly luminescent ZnCdTeS nanocrystals with wide spectral tunability for efficient color-conversion white-light-emitting-diodes, *J. Phys. D: Appl. Phys.* 54 (2021) 505110, <https://doi.org/10.1088/1361-6463/ac26f5>.
- [60] L. Chen, X. Tian, Y. Zhao, Y. Li, C. Yang, Z. Zhou, X. Liu, A ratiometric fluorescence nanosensor for highly selective and sensitive detection of selenite, *Analyst* 141 (2016) 4685–4693, <https://doi.org/10.1039/C6AN00740F>.
- [61] X. Wei, M. Meng, Z. Song, L. Gao, H. Li, J. Dai, Y. Yan, Synthesis of molecularly imprinted silica nanospheres embedded mercaptosuccinic acid-coated CdTe quantum dots for selective recognition of λ-cyhalothrin, *J. Lumin.* 153 (2014) 326–332, <https://doi.org/10.1016/j.jlumin.2014.03.055>.
- [62] M.C. Sekhar, A. Samanta, Ultrafast transient absorption study of the nature of interaction between oppositely charged photoexcited CdTe quantum dots and cresyl violet, *J. Phys. Chem. C* 119 (2015) 15661–15668, <https://doi.org/10.1021/acs.jpcc.5b02203>.
- [63] G.P. Murphy, X. Zhang, A.L. Bradley, Temperature-dependent luminescent decay properties of CdTe quantum dot monolayers: impact of concentration on carrier trapping, *J. Phys. Chem. C* 120 (2016) 26490–26497, <https://doi.org/10.1021/acs.jpcc.6b04734>.
- [64] A. Badawi, N. Al-Hosiny, S. Abdallah, S. Negm, H. Talaat, Tuning photocurrent response through size control of CdTe quantum dots sensitized solar cells, *Sol. Energy* 88 (2013) 137–143, <https://doi.org/10.1016/j.solener.2012.11.005>.
- [65] O. Madelung, *Semiconductors: Data Handbook*, Springer Science & Business Media, 2012.
- [66] T. Trindade, P. O'Brien, N.L. Pickett, Nanocrystalline semiconductors: synthesis, properties, and perspectives, *Chem. Mater.* 13 (2001) 3843–3858, <https://doi.org/10.1021/cm000843p>.
- [67] D.H. Nguyen, S.H. Kim, J.S. Lee, D.S. Lee, H.S. Lee, Reaction-dependent optical behavior and theoretical perspectives of colloidal ZnSe quantum dots, *Sci. Rep.* 14 (2024) 13982, <https://doi.org/10.1038/s41598-024-64995-5>.
- [68] R.B. Laughlin, Optical absorption edge of SiO<sub>2</sub>, *Phys. Rev. B* 22 (1980) 3021–3029, <https://doi.org/10.1103/PhysRevB.22.3021>.

- [69] A. Ruivo, C. Laia, CIE color coordinates for the design of luminescent glass materials, *Color Res. Appl.* 49 (2024) 199–214, <https://doi.org/10.1002/col.22907>.
- [70] Z. Liu, B. Yang, C. Zhang, Y. Li, J. Zou, M. Shi, X. Qian, F. Zheng, Model prediction on the correlated color temperature of white LED based on chromaticity coordinate, *J. Lumin.* 216 (2019) 116652, <https://doi.org/10.1016/j.jlumin.2019.116652>.
- [71] D.S. Daibagya, Spectral and kinetic characteristics of ultrathin cadmium selenide nanoscrolls, *Sci. Tech. J. Inf. Technol. Mech. Opt.* 23 (2023) 920–926, <https://doi.org/10.17586/2226-1494-2023-23-5-920-926>.